Giant Quantum Oscillations in Gallium*

N. K. Batra and R. L. Thomas
Department of Physics, Wayne State University, Detroit, Michigan 48202
(Received 14 March 1973)

Giant quantum oscillations (GQO) are reported in both the electromagnetic-sound-generation efficiency and the ultrasonic attenuation for propagation along the $\vec{a}$, $\vec{b}$, and $\vec{c}$ crystallographic directions in gallium in a longitudinal magnetic field. With the exception of shear waves propagating along $\vec{b}$, GQO were observed for all sound polarization directions for this geometry. The GQO periods and corresponding effective masses obtained from these measurements are in good agreement with those found in the literature. Conduction-electron g values are deduced from spin splitting for the first time along the $\vec{a}$ and $\vec{c}$ directions. In many cases the oscillations are more pronounced in the generation, and by suitable rf-coil orientation a single GQO period can be made dominant. This extra degree of rotational freedom makes electromagnetic sound generation a very useful technique for the experimental determination of a variety of band-structure parameters.

I. INTRODUCTION

Giant quantum oscillations (GQO) in the ultrasonic attenuation in a pure metal at very low temperatures were first predicted theoretically by Gurevich, Skobov, and Firsov[1] and were first observed experimentally in bismuth by Korolyuk.[2] Shortly thereafter, GQO were observed by Shapira[3] in gallium. Shapira and his collaborators have since investigated several different aspects of these experiments quantitatively.[4–6] More recently, Dobbs, Thomas, and Hsu[7] observed experimentally that GQO also are present in the conversion efficiency of electromagnetic sound generation in bismuth. This experiment, as well as subsequent work by Hsu and Thomas,[8] indicated that the GQO effects can be considerably more pronounced in the generation process than in the attenuation of the propagating wave.

In this paper we present experimental observations of GQO in both the electromagnetic generation efficiency and the attenuation of sound waves in gallium. We extend the earlier attenuation measurements of Shapira[3–6] to include both shear wave and longitudinal wave propagation along all three high symmetry directions. From these data we determine values of conduction-electron g factors for the first time with the magnetic field along the $\vec{a}$ and $\vec{c}$ axes. In addition, we observe essentially all of the de Haas-van Alphen periods reported in the literature for the three principal directions and are able to assign cyclotron effective masses to a number of these periods from measurements of the GQO line shapes. It is demonstrated by this example in gallium that the new technique of using a rotatable coil to generate the sound waves offers a number of practical advantages for experimental determination of a variety of band-structure parameters. For instance, the GQO are not only usually more pronounced in the generation efficiency, but also can be simplified considerably by proper rf-coil orientation. In turn, the GQO themselves have linewidths and spin-splitting which are readily related to the corresponding cyclotron effective masses and g factors, respectively.

II. EXPERIMENTAL TECHNIQUE

Two single-crystal specimens were used in the present measurements. They were grown by directional seeding from the melt starting with 99.9999+% nominal purity gallium metal.[9] Specimen B-6 was grown with two sets of plane parallel faces: one set normal to the $\vec{a}$ axis was spaced 1.31 cm apart, the other set normal to the $\vec{b}$ axis was spaced 1.61 cm apart. Specimen B-9 was grown with a set of faces normal to the $\vec{c}$ axis, spaced 1.51 cm apart.

Pulse-echo techniques were employed, using a coil to generate and a quartz transducer to receive the sound pulse when studying the generation, and utilizing the quartz transducer for both conversions when studying the ultrasonic attenuation. The quartz transducer was always bonded to the same face for a given direction of propagation, using silicone fluid as a bonding agent. Most of the measurements were made using a superconducting solenoid, with the direction of sound propagation being along the magnetic field. A sample holder was employed[10] which allowed the rf coil to be rotated in a plane parallel to that of the sample face. Measurements of GQO were made over the frequency range 10–50 MHz, and in some cases up to 300 MHz.

III. THEORY

The theoretical treatments for the GQO periods, line shape, amplitude, and spin-splitting have been reviewed by Shapira[5] for the case of the ultrasonic attenuation. Since the background changes

are reasonably slowly varying functions of magnetic field, it seems reasonable to expect that similar results should hold for the periods, line shapes, and spin splittings observed in the electromagnetic generation efficiency. A necessary (but perhaps not sufficient) condition for observation of GQO is[5] $B \equiv (2kT/m^*)^{1/2} q\tau \gg 1$, while sufficient conditions are[5] $B \gg 1$; $\omega\tau \gg 1$. Here, q and ω are the wave number and angular frequency of the sound wave, m^* is the effective mass of the carriers, k is Boltzmann's constant, and τ is the electronic relaxation time, which is estimated from other measurements[11] to be $\tau \approx 3\times10^{-9}$ sec at $T = 1.2$ K. For these samples at 10 MHz and $T = 1.2$ K we estimate that typically $B \sim 4$ and $\omega\tau \sim 0.3$. Since both m^* and τ depend on the group of electrons (holes) under consideration, it is possible for the condition $B > 1$ to be violated for one group of carriers under the same conditions for which it is satisfied for another group. It has been pointed out[5] that a useful indication of the unimportance of collision broadening is that all linewidths be independent of frequency. This was observed to be the case for all the present data, with the exception of very slight broadening of the $\vec{a}$-axis data at 10 MHz. In all cases only data taken for frequencies higher than 20 MHz were used to estimate effective masses, and in this frequency range no collision broadening was observed.

For the geometry chosen for these experiments, and for intra-Landau level electron-phonon scattering, the period in B_0^{-1} of the GQO is very close to that of the de Haas-van Alphen effect,

$$P = 2\pi e/\hbar c A_{ex} \tag{1}$$

where A_{ex} is the extremal cross-sectional area of the Fermi surface which is normal to the magnetic field. From the full width $(\delta B_0)_n$ at half-maximum of the nth GQO, one may determine the effective mass from the following relationship[3]:

$$(\delta B_0)_n = 3.53\left(\frac{kTB_{0_n}P}{\mu_B}\right)\frac{m^*}{2m_e}, \tag{2}$$

where

$$\mu_B = e\hbar/2m_e c\ .$$

In several of the experimental traces which will be presented in Sec. IV, structure is evident in the high field GQO which is identified as being due to spin splitting of Landau levels. An alternative description might be considered in terms of two close, but nonidentical, GQO periods being superimposed. As has been pointed out earlier by Shapira,[4] however, this possibility is easily ruled out experimentally for the case of reasonably low Landau level number, $n = (PB_{0_n})^{-1}$, as such a situation would lead to different values of g when adjacent (assumed) spin-split GQO are analyzed according to the expression[4]

$$g = \frac{2m_e}{m^*}\left(\frac{B_0' - B_0}{PB_0'B_0} + l\right). \tag{3}$$

Here, m_e is the mass of a free electron, B_0' and B_0 are the subpeaks of the spin-split GQO, and l is an integer, most likely to be 0, corresponding to the case in which the two subpeaks arise from electrons in the same Landau level. It should be noted that in analyzing the GQO line shape to estimate the effective mass, it is desirable to examine a well-resolved spin-split subpeak at very high fields.

IV. RESULTS

A. Sound Propagation along the $\vec{a}$ Axis

The utility of having extra degrees of freedom associated with the relative rf-coil orientation when measuring electromagnetic generation efficiencies is well illustrated in the $\vec{a}$-axis longitudinal wave traces displayed in Figs. 1 and 2. The attenuation GQO are rather complicated, as is the generation signal when $\vec{E}_{rf}$ (the component of the rf electric field in the plane of the sample face) is along the $\vec{c}$ axis (Fig. 1). For $\vec{E}_{rf}$ along the $\vec{b}$ axis, however, a nearly pure GQO period (19.7×10^{-7} G^{-1}) is seen in the generation (Fig. 2), which in turn can be used to identify the same period in Fig. 1. Subsequent analysis leads to the identification of the second set of Landau levels designated in Fig. 1. None of the high-field peaks in this configuration are noticeably spin split at these fields. It is interesting to note that in this

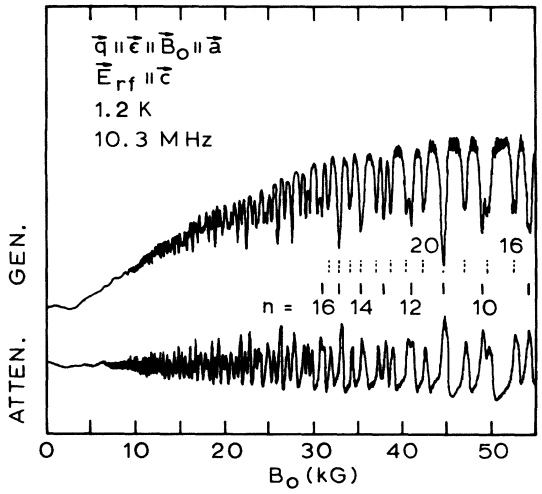

FIG. 1. Recorder tracing of the one pass generation ($\vec{E}_{rf} \parallel \vec{c}$) and six pass attenuation of 10.3-MHz longitudinal waves in gallium at 1.2 K with $\vec{q} \parallel \vec{B}_0 \parallel \vec{a}$. There are two identifiable periods present: (1) 19.7×10^{-7} G^{-1} with highest field (minimum) Landau level $n = 9$; (2) 11.3×10^{-7} G^{-1} with minimum $n = 16$.

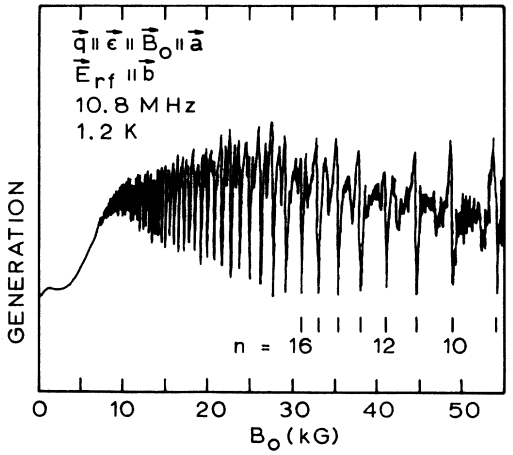

FIG. 2. Recorder tracing of the three pass 10.8-MHz longitudinal wave generation for $\vec{E}_{rf} \parallel \vec{b}$ with $\vec{q} \parallel \vec{B}_0 \parallel \vec{a}$. Note that orienting $\vec{E}_{rf}$ along $\vec{b}$ singles out a pure period (19.7×10^{-7} G^{-1}) from among those present in Fig. 1 for the same direction of propagation along $\vec{B}_0$. The small amplitude oscillations at high fields have a period of 0.412×10^{-7} G^{-1}.

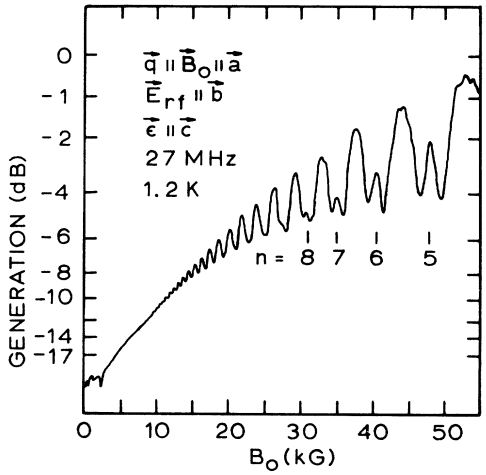

FIG. 3. Recorder tracing of the one pass slow shear wave generation for $\vec{E}_{rf} \parallel \vec{b}$ (ξ_y) with $\vec{q} \parallel \vec{B}_0 \parallel \vec{a}$. A pure GQO period ($40.6 \times 10^{-7}$ G^{-1}) is present which shows spin splitting at high fields.

geometry ($\vec{q} \parallel \vec{B}_0$) the Lorentz force on the rf eddy currents which would give rise classically to a compressional strain is zero.

Similar measurements were made of the shear wave generation and attenuation both for the fast shear ($\vec{\epsilon} \parallel \vec{b}$) and slower shear ($\vec{\epsilon} \parallel \vec{c}$) polarizations. Several new periods were seen, although one of the dominant periods from the longitudinal trace (11.3×10^{-7} G^{-1}) was not observed in any of the shear wave traces. Figure 3 is illustrative of the slow shear wave generation GQO, and shows spin splitting for $B_0 > 25$ kG. The same nearly pure period with comparable spin splitting was also observed in the slow shear wave attenuation along the $\vec{a}$ axis.

B. Sound Propagation along the $\vec{b}$ Axis

Shapira's measurements[3-6] were made primarily on longitudinal GQO in the attenuation for this configuration. Our longitudinal GQO in the attenuation, measured in the range 10–190 MHz, were very similar to Shapira's[3-6] higher field traces. In addition, we observed GQO's in the longitudinal wave electromagnetic generation. For shear wave propagation along the $\vec{b}$ axis, *no* GQO were observed in the attenuation or the generation of either the fast or slow shear wave modes. Except for a few oscillations at low fields (Doppler shifted cyclotron resonance),[11] the attenuation was practically flat up to 55 kG, and the generation increased monotonically with B_0. As this was the same sample (B-6) used for the measurements described above for propagation along the $\vec{a}$ axis, it would seem that the free-electron model selection rule ($\Delta n = \pm 1$ for shear waves with $\vec{q} \parallel \vec{B}_0$) holds for this set of carriers and that $\omega\tau$ is not sufficiently large to observe such transitions.

C. Sound Propagation along the $\vec{c}$ Axis

As was the case for propagation along the $\vec{a}$ axis, the longitudinal wave attenuation was complicated, with several periods superimposed. The electromagnetic generation with $\vec{E}_{rf}$ along $\vec{b}$, however, was both more pronounced and greatly simplified. Although a fast period oscillation was seen at high fields, there was no evidence of spin splitting for

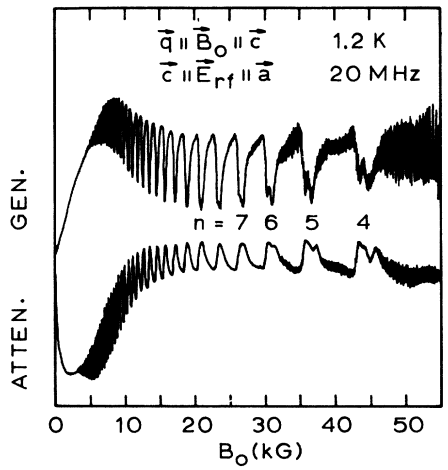

FIG. 4. Recorder tracing of the one pass generation (ξ_x) and two pass attenuation of shear waves with $\vec{q} \parallel \vec{B}_0 \parallel \vec{c}$. In both cases a pure long period (50.8×10^{-7} G^{-1}) dominates and shows spin splitting at high fields. It can be seen that the GQO are more pronounced in the generation for this period. Additional short periods (1.17×10^{-7} G^{-1} and 0.78×10^{-7} G^{-1}) are seen at high fields.

the longitudinal wave generation or attenuation.

GQO were seen both in the attenuation and generation of shear waves (Fig. 4), being more pronounced for the generation. Spin splitting was apparent for $B_0 > 25$ kG, although somewhat obscured at top field by the strong fast period oscillations.

D. Summary of GQO Periods

In addition to the GQO measurements described above, low-field quantum oscillations were studied with $\vec{B}_0$ nearly normal to $\vec{q}$. The results of all the ultrasonic quantum oscillation periods are summarized in Table I, together with those previously reported for these symmetry directions by several other workers. It can be seen that there is good internal agreement of the high-field and low-field periods in the present work, as well as good agreement with values reported by other workers.

E. Cyclotron Masses and g Factors

In those cases for which well-defined GQO of a single period could be identified, after determining the periods as summarized above, estimates were made of the corresponding cyclotron effective masses and g factors using Eqs. (2) and (3), respectively. The results are given in Table II.

The GQO for shear waves propagating parallel to the magnetic field and along the $\vec{a}$ axis, [$P = (40.6 \pm 0.3) \times 10^{-7}$ G^{-1}], showed spin splitting at high fields (see Fig. 3). Using the expressions given in Sec. III, we find an effective mass from these oscillations of $m^*/m_e = 0.35 \pm 0.02$, which compares very well with Moore's[15] value for his branch M along the $\vec{a}$ axis. This set of carriers also apparently was observed as the dominant signal in *acoustic* cyclotron resonance by Lewiner[16] (his branch I in the ab plane), and by Alquié and Lewiner[17] (branch C_4). The g factor deduced from the spin splitting of these GQO (assuming $l = 0$) is $|g| = 1.7 \pm 0.1$. Our estimate of $m^*/m_e = 0.15$ for $P = 19.7 \times 10^{-7}$ G^{-1} is also in good agreement with Moore's[15] $\vec{a}$ axis branch B, and our estimate $m^*/m_e = 0.32$ for $P = 11.3 \times 10^{-7}$ G^{-1} has no apparent counterpart in Moore's[15] data.

The GQO for longitudinal waves propagating parallel to the magnetic field and along the $\vec{b}$ axis, $P = (29.5 \pm 0.3) \times 10^{-7}$ G^{-1}, yielded $m^*/m_e = 0.063 \pm 0.008$. This agrees very well with the measurements by Shapira and Lax[5] of the four oscillations between 60 and 140 kG. Their analysis by computer fitting the field and temperature dependence of the entire linewidth including spin splitting gave a value of

TABLE I. Comparison of de Haas-van Alphen periods in gallium (units of 10^{-7} G^{-1}).

Axis	This work[a]	Goldstein and Foner[b] Rotation		On Axis	Shoenberg[c]	Shapira and Lax[d]	Lyall and Cochran[e]
	40.6 ± 0.3[f]				41.66		
	27.4 ± 0.2						
$\vec{a}$	19.7 ± 0.2	20.2	19.8	20.0	20.0		19.65
	19.6 ± 0.1[g]						
	11.3 ± 0.3[h]	11.69	11.56	11.49	10.98		
	0.412 ± 0.004	0.426	0.431	0.435			
	29.5 ± 0.3[h]	28.98	29.85	29.24	30.3	29.8 ± 1.5	29.59
	29.4 ± 0.1[g]						
$\vec{b}$	13.7 ± 0.3	13.79	13.6			14	
	0.53 ± 0.01	0.52	0.535	0.526		0.55	
	0.31 ± 0.02	0.333	0.333	0.326			
	50.8 ± 0.8[f]						
	50.4[g]	50.0	50.0		50.0		
	47.7			47.8		47.62	
$\vec{c}$	45.1 ± 0.8	45.45	44.44	43.10	45.45		45.45[i]
	45.0 ± 0.8[g]					12.05	
	13.0 ± 0.2[h]	13.07	13.15	13.15			
	1.17 ± 0.01	1.2	1.176	1.176			
	0.78 ± 0.02	0.769	0.781	0.781			

[a]High field GQO, $\vec{q} \parallel \vec{B}_0$.
[b]Reference 12.
[c]Reference 13.
[d]Reference 5 (GQO).
[e]Reference 14 (sound velocity quantum oscillations).
[f]Not seen in longitudinal wave GQO.
[g]Low-field GQO, $\vec{q} \perp \vec{B}_0$.
[h]Not seen in shear wave GQO.
[i]Reference 14 (skin depth quantum oscillations).

TABLE II. Estimates of cyclotron effective masses and g factors using Eqs. (2) and (3).

Axis	P (in units of 10^7 G)	m^*/m_e GQO	m^*/m_e Moore[b] (branch)	g factor[a] This work	g factor[a] Shapira[c]
	40.6	0.35	0.347 (*M*)	1.7 ± 0.1	
$\vec{a}$	19.7	0.15[d]	0.154 (*B*)		
	11.3	0.32			
	29.5	0.063	0.0513 (*C*)	0.7 ± 0.1	0.95 ± 0.11
$\vec{b}$	13.7	0.27			
	50.8	0.13	0.140 (*M'*)	1.9 ± 0.3	
$\vec{c}$	13.0	0.43[d]	0.437 (*U*)		

[a]Calculated assuming GQO values for m^*/m_e
[b]Reference 15.
[c]Reference 4.
[d]Analyzed from the generation data.

$m^*/m_e = 0.065 \pm 0.005$, close to Moore's[15] value for his branch C ($m^*/m_e = 0.051$). The spin splitting observed in the present work for this direction was barely resolved at 50 kG, yielding a value of $|g| = 0.7 \pm 0.1$, in reasonable agreement with Shapira's estimate of $|g| = 0.95 \pm 0.11$ (again it is assumed that $l = 0$). The small splitting is responsible for the larger uncertainty for $|g|$ from these data. Alquié and Lewiner[17] have also apparently observed this set of carriers by acoustic cyclotron resonance, but with considerably greater experimental uncertainty, and they also identify this branch ($A5$) in the bc plane with Moore's[15] branch C. The other mass ($m^*/m_e = 0.27$) which we estimate along $\vec{b}$ for $P = 13.7 \times 10^{-7}$ G^{-1} has no apparent counterpart in Moore's[15] data.

The GQO for shear waves propagating parallel to the magnetic field and along the $\vec{c}$ axis, $P = (50.8 \pm 0.8) \times 10^{-7}$ G^{-1}, yielded $m^*/m_e = 0.13 \pm 0.02$, which is close to Moore's[15] value of $m^*/m_e = 0.140$ for his branch M', as well as Alquié and Lewiner's[17] branch $A6$. Analysis of the spin splitting of the $n = 4$ level (assuming $l = 0$) yielded $|g| = 1.9 \pm 0.3$. Our estimate of $m^*/m_e = 0.43$ for $P = 13.0 \times 10^{-7}$ G^{-1} suggests that this corresponds to Moore's[15] branch U.

V. DISCUSSION

We have presented GQO data for sound propagation along each of the high symmetry directions in gallium. In each case, the oscillations are present in the electromagnetic sound generation efficiency wherever they are present in the attenuation. With the exception of the $\vec{b}$ axis, for which none were observed in shear wave generation or attenuation, GQO were observed for all possible sound polarizations. In general, the GQO could be greatly simplified in the generation by a judicious orientation of the rf fields, and were usually simpler for the shear wave configurations than for longitudinal waves. Usually different groups of electrons dominated the GQO for shear waves than for longitudinal waves, and the composite set of periods was seen to include nearly all those previously reported in de Haas-van Alphen effect studies (see Table I).

The absence of observable shear wave GQO along $\vec{b}$ in a longitudinal magnetic field at the frequencies utilized in this work suggests that the free-electron model selection rule $\Delta n = \pm 1$ holds for this geometry. We estimate that for $\tau \sim 3 \times 10^{-9}$ sec, appropriate to these samples, $\Delta n = \pm 1$ GQO may be observable at x-band ultrasonic frequencies. Experiments are presently underway to search for such oscillations, which should be related[18] to nonextremal cross sections of the Fermi surface of gallium.

We have observed spin splitting in the shear wave GQO along $\vec{a}$ and $\vec{c}$, as well as in the longitudinal wave GQO along $\vec{b}$, which was previously reported by Shapira.[5] We have deduced for the first time g factors for groups of electrons which interact strongly with shear sound waves along $\vec{a}$ and $\vec{c}$. Additionally, from the line shapes of the GQO we have deduced the effective masses corresponding to a number of these periods and find values which are in reasonable agreement with ones observed in cyclotron resonance experiments.[15,17]

In summary, the application of electromagnetic sound generation techniques to GQO studies has been demonstrated to be very useful in the determination of a variety of band-structure parameters in a metal which has a complicated Fermi surface such as gallium.

ACKNOWLEDGMENTS

The authors are grateful to Professor A. M. de Graaf and K. C. Lee for useful discussions.

*Research sponsored by the U. S. Air Force Office of Scientific Research, Office of Aerospace Research under AFOSR Grant No. AFOSR-71-1965D.

[1]V. L. Gurevich, V. G. Skobov, and Yu. A. Firsov, Zh. Eksp. Teor. Fiz. **40**, 786 (1961) [Sov. Phys.-JETP **13**, 552 (1961)].
[2]A. P. Korolyuk, Fiz. Tverd. Tela **5**, 3323 (1963) [Sov. Phys.-Solid State **5**, 2433 (1964)].
[3]Y. Shapira and B. Lax, Phys. Rev. Lett. **12**, 166 (1964).
[4]Y. Shapira, Phys. Rev. Lett. **13**, 162 (1964).
[5]Y. Shapira and B. Lax, Phys. Rev. **138**, A1191 (1965); Y. Shapira, in *Physical Acoustics*, edited by Warren P. Mason (Academic, New York, 1968), Vol. V.
[6]Y. Shapira and L. J. Neuringer, Phys. Rev. Lett. **18**, 1133 (1967).
[7]E. R. Dobbs, R. L. Thomas, and D. Hsu, Phys. Lett. A **30**, 338 (1969).
[8]D. Hsu and R. L. Thomas, Phys. Rev. B **5**, 4668 (1972).
[9]Obtained from Alcoa, 1501 Alcoa Building, Pittsburgh, 19 Pa.
[10]G. Turner, R. L. Thomas, and D. Hsu, Phys. Rev. B **3**, 3097 (1971).
[11]N. K. Batra, Ph.D. thesis (Wayne State University, 1972) (unpublished); Bull. Am. Phys. Soc. **18**, 94 (1973).
[12]Albert Goldstein and Simon Foner, Phys. Rev. **146**, 442 (1966).
[13]D. Shoenberg, Philos. Trans. R. Soc. Lond. A **245**, 1 (1952).
[14]K. R. Lyall and J. F. Cochran, Can. J. Phys. **49**, 1075 (1971).
[15]T. W. Moore, Phys. Rev. **165**, 864 (1968).
[16]J. Lewiner, Phys. Rev. Lett. **19**, 1037 (1967).
[17]C. Alquié and J. Lewiner, Phys. Rev. B **6**, 4490 (1972).
[18]J. J. Quinn, Phys. Rev. **137**, A889 (1965).